CrossMark

ORIGINAL ARTICLE

Verification of tropical cyclone heat potential for tropical cyclone intensity forecasting in the Western North Pacific

Akiyoshi Wada[1]

Abstract Tropical cyclone heat potential (TCHP) is a measurable metric calculated by the summation of ocean heat content from the surface down to the depth of the 26 °C isotherm. TCHP calculated by the Meteorological Research Institute multivariate ocean variational estimation (MOVE) system is verified by using TCHP based on in situ observations by profiling floats during 2002–2012. After the verification, the threshold of MOVE-based TCHP before the passage of a tropical cyclone (TC) favorable for triggering TC deepening is determined by best-track central pressure drops for the nearest 6 hours from 1985 to 2012. The threshold is specified as the minimum range of TCHP when the ratio of the number of records for TC deepening to the total best-track number of records in a TCHP bin is significantly greater than the reference ratio determined for each domain at a significance level of 0.05. The threshold is relatively low (40–60 kJ cm^{-2}) around 5–10°N, west of 120°E and east of 140°E, whereas it is relatively high (80–100 kJ cm^{-2}) around 15–20°N. Around 5–10°N, the ratio for each moving speed shows two peaks: with moving speeds of 3–5 and 7–9 m s^{-1}. The former case is exemplified by Typhoon Mike (1990) under relatively low TCHP (< 80 kJ cm^{-2}), whereas the latter case is exemplified by Typhoon Haiyan (2013), which is more rapidly intensified and reaches a lower minimum central pressure under relatively high TCHP (>120 kJ cm^{-2}).

1 Introduction

Accurate tropical cyclone (TC) forecasting is indispensable for mitigating the disastrous impacts caused by TCs. To improve TC forecasting, the development of prediction with sophisticated numerical models is desirable. However, our current understanding of TC intensity prediction has been limited because of the insufficient horizontal resolution of numerical models; lack of understanding of atmospheric and oceanic physical processes; lack of in situ observations, particularly around a TC; and uncertainties regarding the roles of pre-existing atmospheric and oceanic conditions in TC intensification and the maximum TC intensity (e.g., Wang and Wu 2004).

It is known that not only sea surface temperature, but also vertical profiles of water temperature and salinity play a crucial role in TC intensity prediction with atmosphere–ocean coupled models. TCs usually intensify when they pass over the western Pacific warm pool (Wang and Zhou 2008; Wada and Chan 2008), the Subtropical Countercurrent region in the western North Pacific (Lin et al. 2005; Wada and Usui 2007), and warm-core eddies in the North Atlantic (Shay 2010).

Recent studies have reported on the relationships between tropical cyclone heat potential (TCHP) and TC intensification and between TCHP and TC maximum intensity. TCHP is a measurable metric calculated by the summation of ocean heat content from the surface down to the depth of the 26 °C isotherm (Leipper and Volgenau 1972). The TCHP value is calculated by using the following equation:

✉ Akiyoshi Wada
awada@mri-jma.go.jp

[1] Meteorological Research Institute, 1-1 Nagamine, Tsukuba, Ibaraki 305-0052, Japan

Springer

$$Q = c_p \sum_{z=0}^{Z26} \rho_i(T_i - 26)\Delta z_i, \tag{1}$$

where Q is the TCHP value (J cm^{-2}), c_p is specific heat at constant pressure, T_i is water temperature in °C at the i-th level, Δz_i is i-th layer water thickness, and ρ_i is the density of water at the i-th level. The parameter Z26 is the depth (m) of the 26 °C isotherm. The relationships between TCHP and TC intensification or TC deepening, and between TCHP and TC maximum intensity, have been studied in the North Atlantic Ocean (Shay et al. 2000; Goni and Trinanes 2003; Goni et al. 2009; Mainelli et al. 2008; Law 2011; Gjorgjievska and Raymond 2014), the Indian Ocean (Ali et al. 2007, 2012; Lin et al. 2009a; Kumar and Chakraborty 2011; Malan et al. 2013; Vissa et al. 2013), and the Pacific Ocean (Pun et al. 2007, 2013, 2014; Wada and Usui 2007; Wada and Chan 2008; Shay and Brewster 2010; Knaff et al. 2013; Wada et al. 2012).

According to Wada and Usui (2007), changes in TCHP values were coincident with those of central pressures during the decaying phase of two typhoons, Typhoons Chaba and Songda, in 2004. Wada and Usui (2010) reported that Typhoon Hai-Tang in 2005 rapidly intensified when the typhoon passed over two warm core eddies. Over the warm oceans with high TCHP, the supply of moisture from the ocean increases in the tropical cyclone boundary layer through vertical advection and stretching, as a result of the release of filamentation, the formation of mesovortices, and vortex merger events under favorable atmospheric conditions (e.g., Wada 2009; Wada et al. 2013). Gray (1979) emphasized the need for warm oceans to a depth to provide the necessary heat to support the cyclogenesis as a threshold against its tendency to cool the ocean by upwelling and turbulent mixing. The studies have indicated that high TCHP is requisite for TC intensification.

Except for studies with TCHP data sets calculated based on sophisticated oceanic data assimilation systems (Wada and Usui 2007; Wada and Chan 2008; Wada et al. 2012; Malan et al. 2013), most of the studies have used ocean thermal structures derived from a convenient assimilation system based on satellite altimetry and a two-layer reduced gravity model (Goni et al. 1996; Shay et al. 2000; Pun et al. 2007). The ocean thermal structure has been characterized by only two isotherms at depths of 26 m (so called D26) and 20 m (D20). Pun et al. (2014) recently determined various isotherms from 4 to 29 °C at intervals of 1 °C, to estimate TCHP more accurately. However, this method is nothing more than a statistical approach with reference to climatological data.

The Regional Specialized Meteorological Center (RSMC) Tokyo in the Japan Meteorological Agency (JMA) is in charge of the monitoring and forecasting of TCs in the western North Pacific, with an area of responsibility that covers 0–60°N and 100–180°E. In addition, JMA has operated an ocean data assimilation system for monitoring oceanic conditions around Japan, such as the Kuroshio Current, and current climate systems, such as the El Niño-Southern Oscillation, for seasonal predictions. To improve TC intensity forecasts, the TCHP data set, based on the output of the assimilation system, will provide forecasters beneficial information for understanding TC intensity changes and the maximum TC intensity. However, there is no operational guideline for utilizing the TCHP data for TC intensity forecasts, even though a convenient lookup table of the minimum upper-ocean heat content under various translation speeds was reported (Lin et al. 2009b).

The purpose of this study is to provide operational guidelines for utilization of TCHP products, including information regarding a threshold of TCHP that leads to an increase in the occurrence of TC deepening, to improve TC intensity forecasting in the western North Pacific under the assumption of physical processes that TCHP above the threshold plays an essential role in increasing moisture in the tropical cyclone boundary layer, resulting in triggering cumulus convection and thus TC deepening (Gray 1979; Wada 2009; Wada et al. 2013). To develop the guidelines, this study aims to explore the relationship between TCHP and TC deepening for TC moving speeds, TC central pressures, and geographic factors such as longitude and latitude.

This paper is organized as follows. Section 2 explains the data used in this study. Section 3 describes the results and presents discussion about the verification of the TCHP data using in situ observations, the relationship between TC deepening and TCHP below a TC before the passage of the TC, and the effect of geographical factors. In addition, Sect. 3 explores the relationship between TCHP during the passage of the TC and TC development around 5–10°N. Case studies are also presented in Sect. 3. Section 4 is devoted to concluding remarks about this study.

2 Data

2.1 TC best-track data

RSMC-Tokyo TC best-track data from 1985 to 2012 were used in this study (http://www.jma.go.jp/jma/jma-eng/jma-center/rsmc-hp-pub-eg/trackarchives.html). These data include the TC center position, TC central pressure, and 10-minute-average maximum sustained wind speed measured four times a day (at 0600, 1200, 1800, and 2400 UTC). The data include these elements taken eight times a day when a TC is located within 300 km of the coast of Japan, or every hour when a TC makes landfall in Japan. Hereafter, this study mainly uses the best-track data measured
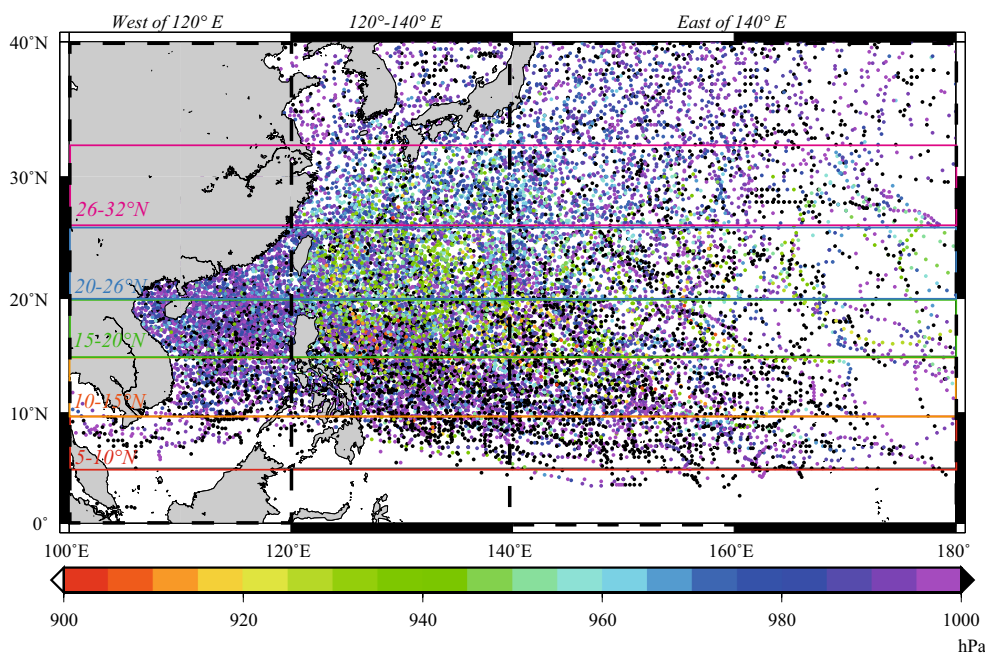
Fig. 1 Horizontal distribution of TC positions obtained from best-track records from 1985 to 2012, with *colors* indicating the RSMC Tokyo best-track central pressure (hPa). *Solid boxes* indicate lati-tudinal analysis domains (5–10°N, 10–15°N, 15–20°N, 20–26°N, 26–32°N). Dashed boxes indicate longitudinal domains (west of 120°E, east of 140°E and 120°–140°E)

four times a day. Figure 1 displays the horizontal distribution of the best-track TC positions used in this study, with colors indicating the central pressure at the position from 1985 to 2012. The number of TC records used in this study is 24,206. Solid and dashed boxes indicate the analysis domain to investigate the relationship between TCHP and TC deepening for TC intensity, TC moving speed and geographical factor.

2.2 Oceanic data set

Daily oceanic reanalysis data are calculated using the North Pacific version of the Meteorological Research Institute multivariate ocean variational estimation (MOVE) system (Usui et al. 2006) for operational monitoring of oceanic environments. The MOVE system incorporates the Meteorological Research Institute community ocean model (MRI.COM: Ishikawa et al. 2005) and a variational analysis scheme to synthesize observations of variables such as sea temperature, salinity, and sea-surface height at different times, locations and measurements, including those performed with satellite altimeters and profiling floats. The domain covers the area from 15°S to 65°N and 100°E to 75°W, with a horizontal resolution of 0.5° and 54 vertical levels. The product archived at JMA consists of 5-day mean historical reanalysis data covering the period since 1985.

The MOVE system has currently applied the three-dimensional variational data assimilation method. The temperature and salinity fields calculated by the ocean general circulation model, the forecasting part of the MOVE system, were modified by the analytical result via an incremental analysis update technique (Usui et al. 2006). The assimilation cycle was 5 days in the MOVE system. This is one of the reasons why the 5-day mean data were used to investigate the relationship between TCHP and TC deepening. Wada et al. (2012) reported that the relationship of the accumulated TCHP, the summation of the TCHP value below a TC before the TC attained the maximum intensity from the genesis, to the minimum central pressure did not depend on the spatial or temporal resolution of the oceanic reanalysis data set, even though the cooling effect of the passage of a TC and the associated decrease in the TCHP values were reproduced realistically only by the daily data set.

Sea temperature and salinity assimilation data were interpolated at 1-m intervals from the subsurface (the uppermost depth of 1 m) to the lowermost depth shallower than 200 m using the method proposed by Akima (1970) to calculate the 5-day TCHP (hereinafter MOVE-based TCHP) and Z26 (hereinafter MOVE-based Z26) before and during the passage of a TC, respectively. MOVE-based TCHP and Z26 were averaged over the square domain of 1.5° centered at the grid corresponding to each TC position from 1985 to 2012. To investigate the relationship between MOVE-based TCHP and TC intensification, Sect. 3.3 used MOVE-based TCHP from 5 days ago as the TCHP data
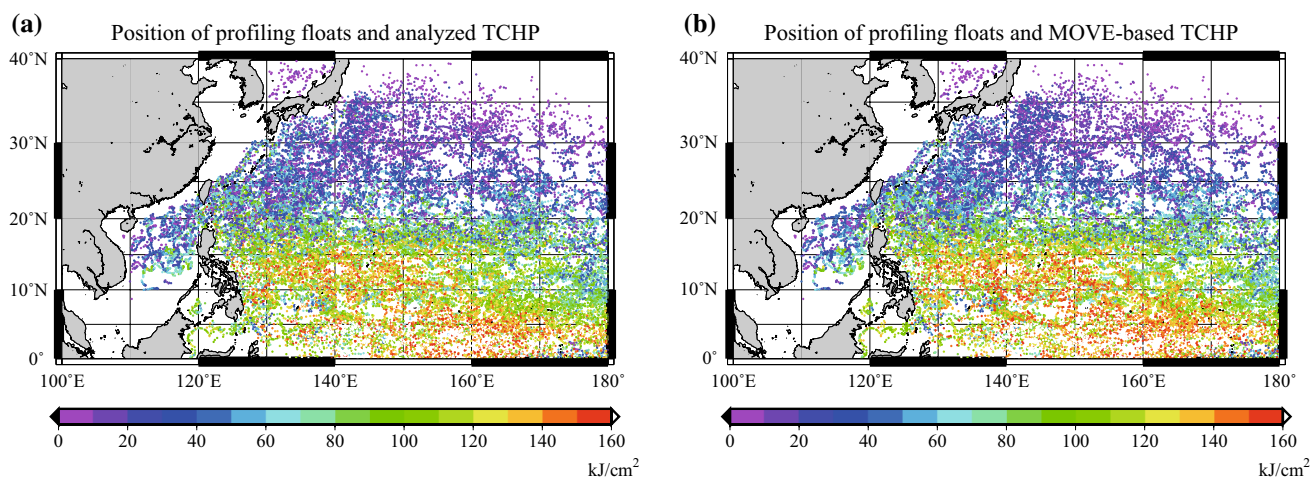
(a)

(b)

Fig. 2 **a** Horizontal distribution of the location of profiling floats from 2002 to 2012, with colors indicating in situ TCHP (kJ cm^{-2}). **b** Horizontal distribution of the location of profiling floats from 2002 to 2012, with *colors* indicating MOVE-based TCHP (kJ cm^{-2})

before the passage of a TC. In Sect. 3.4, the TCHP data during the passage of the TCs was used in order to investigate the relation of the temporal evolution of TCHP and Z26 to TC intensification.

Note that daily operational oceanic data were additionally used for investigating the temporal evolution of daily TCHP and Z26 together with 5-day TCHP and Z26 during the lifetime of Typhoon Haiyan (2013), and for investigating the impact of the temporal resolution on the temporal evolution of TCHP in Sect. 3.4.

2.3 Profiling float data

Profiling float data of sea temperature and salinity during 2002–2012 were used to verify MOVE-based TCHP. Both temperature and salinity data were used to calculate the ocean density, with Eq. 1 based on the equation of state (UNESCO 1981; Gill 1982). The profiling float data were obtained from best-copy data in the Global Temperature and Salinity Profile Program (GTSPP) continuously managed database. Delayed-mode quality control (http://www.jamstec.go.jp/ARGORC/docs_top.html) was applied to the data. The GTSPP data have been currently used in the MOVE system. In that sense, the objective of the verification is to grasp how accurate the MOVE system, with a horizontal resolution of 0.5°, can reproduce the observational characteristic of temperature and salinity at a local point of the observation, which is associated with the estimation of TCHP.

Sea temperature and salinity data by profiling floats were interpolated at 1-m intervals from the subsurface (the uppermost depth of 1 m) to the lowermost depth shallower than 200 m, by using the method proposed by Akima (1970) to calculate the TCHP and Z26 values. Because

there was no surface observation in the profiling floats data, surface sea temperature and salinity were assumed to be equal to the values at the uppermost depth.

2.4 Atmospheric data set

To grasp the relationship of TCHP to the atmospheric environment around 5–10°N in the western North Pacific, the evolutions and variations of specific humidity and geopotential height at 925 hPa from 1985 to 2013 were investigated. These data were provided from monthly products of the Japan Meteorological Agency 55-year Reanalysis data set (JRA-55) with a horizontal resolution of 1.25° (Ebita et al. 2011).

3 Results and discussion

3.1 Verification of TCHP data

First, MOVE-based TCHP (Fig. 2a) was verified using TCHP data calculated from in situ sea temperature and salinity profiles observed by profiling floats from 2002 to 2012 (hereinafter in situ TCHP, Fig. 2b). The number of profiling float data used in this study was 41,867. The horizontal distribution of MOVE-based TCHP was similar to that of in situ TCHP: the TCHP values were relatively high south of 15°N (Fig. 2). Figure 3 shows the relationships between in situ TCHP and MOVE-based TCHP (Fig. 3a), and between Z26 derived from in situ observations (hereafter in situ Z26) and MOVE-based Z26 (Fig. 3b).

The slopes for each regression function were 0.97 and 0.91, and the square of the correlation coefficient was 0.92 for TCHP (Fig. 3a) and 0.88 for Z26 (Fig. 3b), respectively.
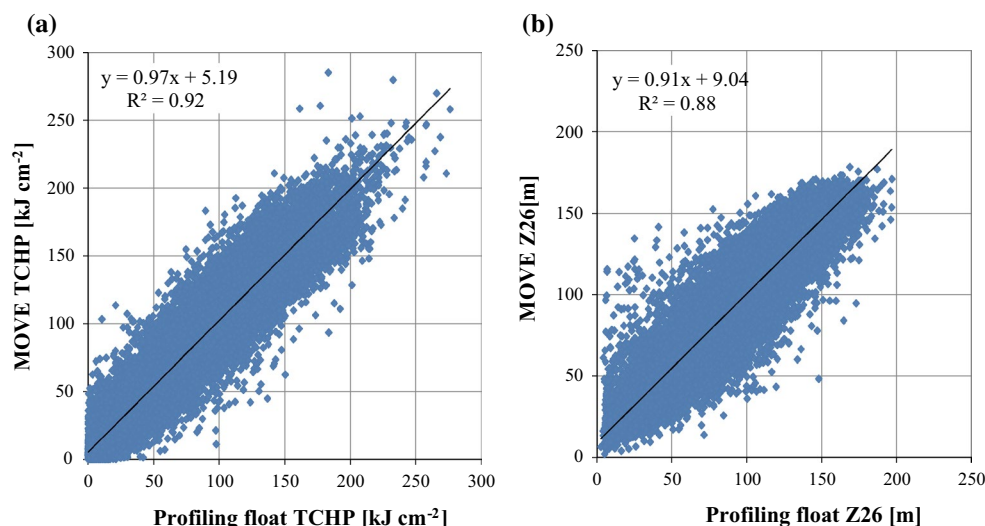
(a)

(b)

Fig. 3 a A scatter diagram of the relationship between in situ TCHP and MOVE-based TCHP, with a regression function (*solid line*). **b** Same as the *left* panel, except for Z26

The intercepts indicate that positive biases existed when in situ TCHP and Z26 were close to zero. In reality, not only the slope, but also the intercept would vary seasonally because of various reasons: frequency of in situ observations; changes of measurement methods, particularly new satellite observations; and issues regarding the assimilation scheme that the MOVE system applied. The slopes indicate that both MOVE-based TCHP and Z26 were lower than in situ TCHP and Z26, as the values of in situ TCHP and Z26 were greater.

The focus is on the temporal evolution of MOVE-based TCHP and Z26 during 2002–2012. Since 2008, MOVE-based TCHP became higher (4 kJ cm^{-2}) compared with TCHP data before 2007 with reference to in situ TCHP (Fig. 4a), while MOVE-based Z26 became deeper (2 m) with reference to in situ Z26 (Fig. 4b) from 2002 to 2012. The stepwise increase in MOVE-based TCHP has occurred just in time for the introduction of Jason-2 satellite altimeter data since 2008 into the assimilation system. This is a specified issue in the MOVE system used in this study.

The relationship between the latitude and the difference between MOVE-based and in situ TCHPs during 2011–2012 indicates that the bias (MOVE-based TCHP minus in situ TCHP) and relative error (defined by the difference divided by the TCHP value) were relatively high at low latitude, whereas the bias was on average equal to zero north of 25°N (Fig. 4c). The characteristics that appeared at low latitude were not found in Z26 (Fig. 4d). In particular, MOVE-based TCHP was extremely high in 2012 compared with in situ TCHP (Fig. 4a): the slope for the regression function was 1.03, and the square of the correlation coefficient was 0.92 (not shown). The relative errors largely scattered north of 15°N, indicating the limitation of the

three-dimensional variational data assimilation method, even though profiling float data were used for the assimilation. However, the spread of the relative errors was small south of 15°N, indicating the existence of systematical biases for MOVE-based TCHP.

The following is the result of verification regarding vertical profiles of water temperature and salinity at low latitude, where the difference between MOVE-based and in situ TCHPs is remarkably large. Figure 5a–c shows vertical profiles of the annual mean MOVE water temperature (Fig. 5a), the standard deviation (Fig. 5b), and the difference in water temperature between the MOVE reanalysis and in situ observation by profiling floats (Fig. 5c) around 5–10°N. The location of the seasonal thermocline shifts downward from 2002 to 2012 (Fig. 5a). The standard deviation is relatively high below Z26 (Fig. 5b). The difference in water temperature between MOVE reanalysis data and in situ observation data by profiling floats becomes high near the seasonal thermocline (at a depth of nearly 80–120 m). In particular, the difference is remarkably high in the seasonal thermocline in 2010 and 2012.

The focus moves on the results of verification regarding vertical profiles of water temperature and salinity at high latitude. Figure 5d–f shows vertical profiles of the annual mean MOVE water temperature (Fig. 5d), the standard deviation (Fig. 5e), and the difference in water temperature between the MOVE reanalysis and in situ observation by profiling floats (Fig. 5f) around 26–32°N. The depth of the mixed-layer base is below 20 m, which is shallower than the depth shown in Fig. 5a. The standard deviation is relatively small above the seasonal thermocline. Unlike the result shown in Fig. 5c, the difference in water temperature between the MOVE reanalysis and in situ observation by
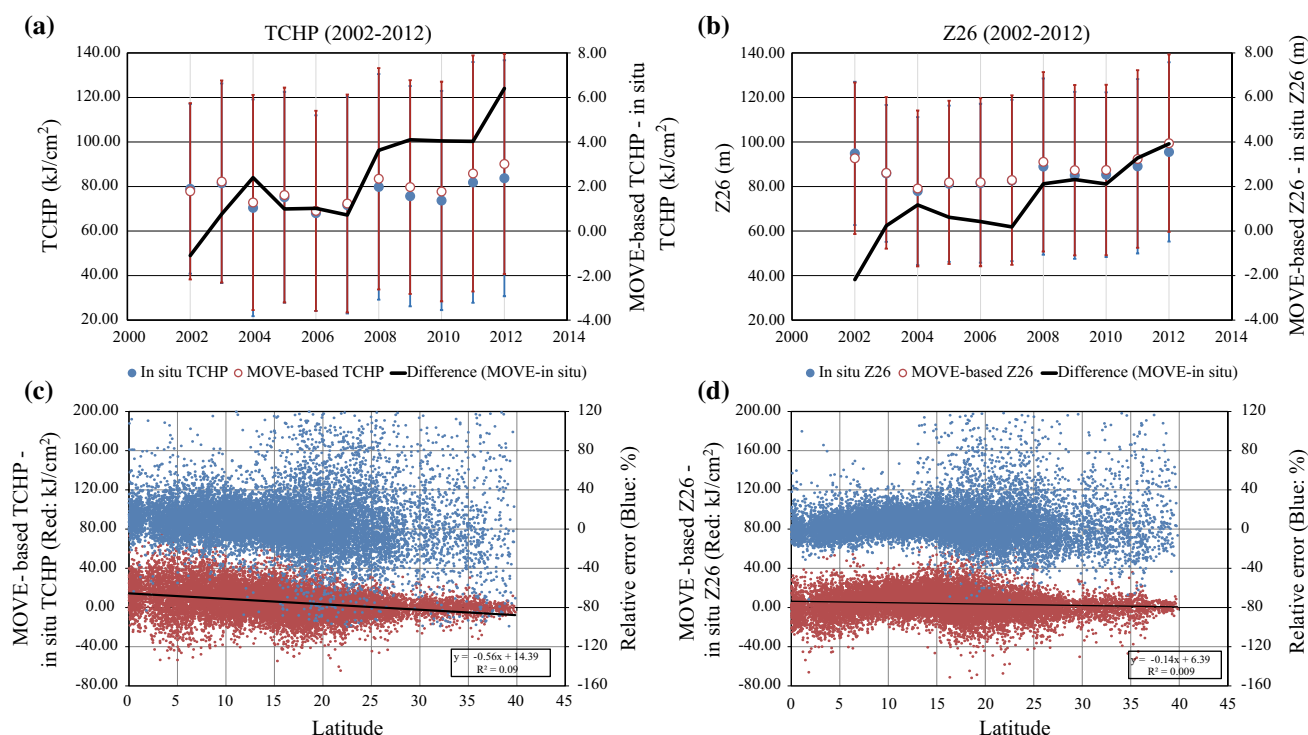
(a)

(b)

(c)

(d)

Fig. 4 **a** Time series of the annual mean MOVE-based (*open brown circles*) and in situ TCHPs (*close blue circles*), with the standard deviation. The *black solid line* indicates the difference between the MOVE-based and in situ TCHPs from 2002 to 2012. **b** Same as (**a**), except for Z26. **c** A scatter diagram of the relation of latitude to the deviation between in situ TCHP and MOVE-based TCHP with the linear regression function for the difference and the error of the difference relative to in situ TCHP. **d** Same as (**c**), except for Z26

profiling floats is relatively small above Z26 (at a depth of nearly 30–40 m). This is the reason why the bias is nearly zero north of 25°N.

In the MOVE system, it is difficult to discuss the effect of the thermal expansion on the long-term trend of TCHP and Z26, even though the trends are statistically significant because of the difficulty to accurately estimate air-sea heat and moisture fluxes including precipitation. Errors of these fluxes involved in the atmospheric forcing directly affect the assimilation of water temperature and salinity. Even though profiling float data are assimilated reasonably well, the error of the estimation of the effect of the thermal expansion possibly leads to poor reproduction of TCHP and Z26 fields, because the number of the data used in the assimilation is very limited.

3.2 Relationship between TCs and TCHP

TCs usually undergo the phases of genesis, development, maturity and decay during their lifetime. As described in Sect. 2.1, this study involved consideration of all 24,206 best-track records for the period from 1985 to 2012. TC deepening is defined here as the positive deviation of TC central pressure ($\Delta p_{6h} > 0$ hPa) for the nearest 6 hours at the corresponding TC record from that at the subsequent

TC record. Δp_{6h} is determined based on RSMC Tokyo best-track data four times a day.

TC deepening is different from TC intensification in that the former is defined by the central pressure, whereas the latter is defined by the maximum sustained wind speed. The number of best-track records for the deviation $\Delta p_{6h} > 0$ was 7052, and the ratio to the total number of records was 29.1 %. The number of records with deviation $\Delta p_{6h} > 5$ hPa was 1126 (4.7 %) and that for $\Delta p_{6h} > 10$ hPa was only 166 (0.7 %).

Figure 6a shows a histogram of the number of best-track records for each bin of MOVE-based TCHP every 20 kJ cm^{-2}. The number of records (7392) is greatest when the TCHP value is 0–20 kJ cm^{-2}, corresponding to approximately 30.5 % of the total number of records. The number for each bin is locally high when the TCHP value is 40–60 kJ cm^{-2} (3561, approximately 14.7 %) and exceeds 100 kJ cm^{-2} (4126, approximately 17 %).

Figure 6b shows cumulative bar charts of the number of records for each TC deepening divided into three bins (0–5, 5–10, and over 10 hPa) for each MOVE-based TCHP every 20 kJ cm^{-2}. In contrast to the result shown in Fig. 6a, the number of records (2035) for TC deepening is greatest when MOVE-based TCHP exceeds 100 kJ cm^{-2} (Fig. 6b). The ratio to the total number of records for TC deepening
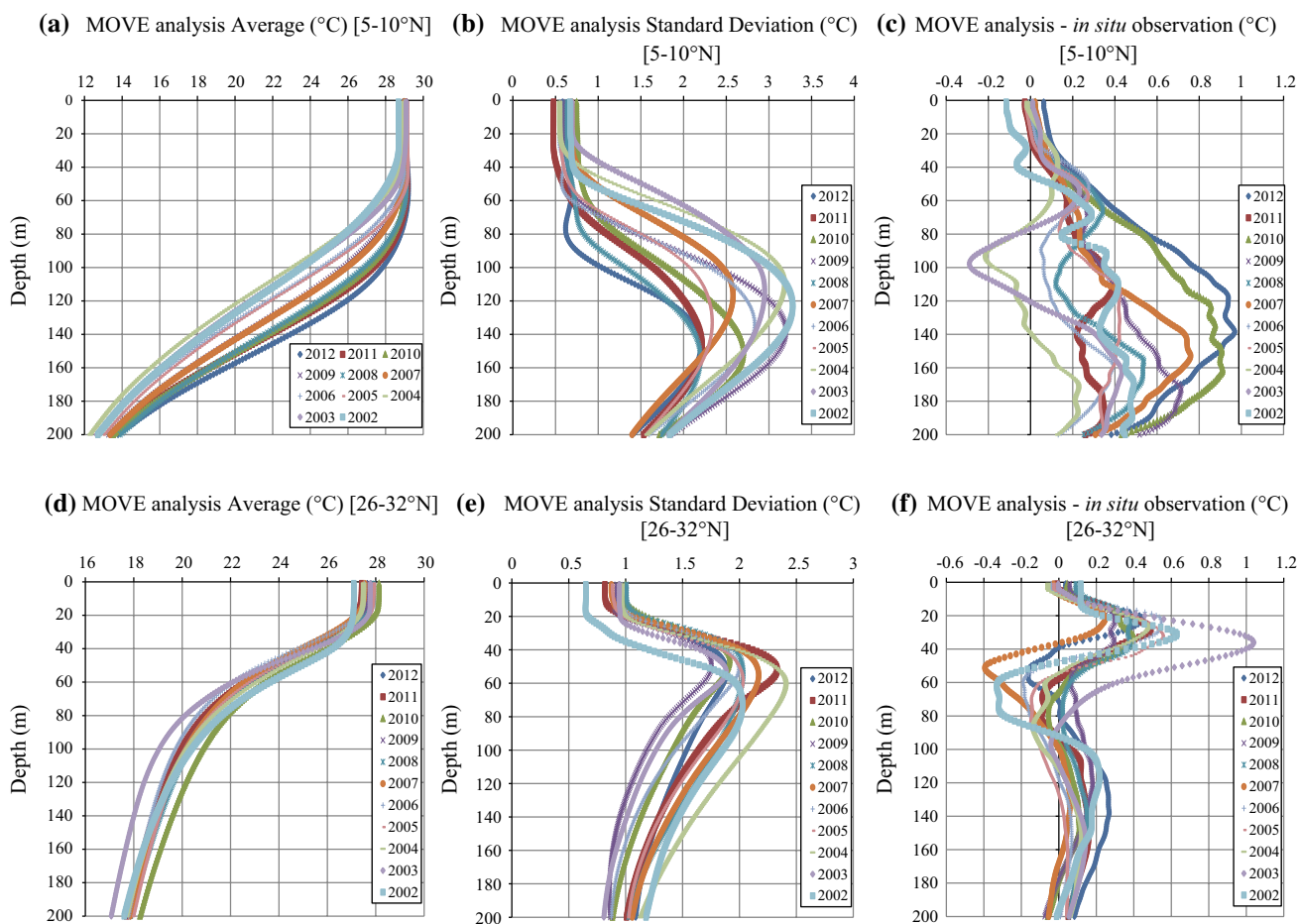
(a) MOVE analysis Average (°C) [5-10°N]   **(b)** MOVE analysis Standard Deviation (°C) [5-10°N]   **(c)** MOVE analysis - *in situ* observation (°C) [5-10°N]

(d) MOVE analysis Average (°C) [26-32°N]   **(e)** MOVE analysis Standard Deviation (°C) [26-32°N]   **(f)** MOVE analysis - *in situ* observation (°C) [26-32°N]

Fig. 5 Vertical profiles of **a** annual mean MOVE water temperature at the corresponding grid to the position of each profile observed by profiling floats around 5–10°N, **b** the standard deviation of MOVE water temperature, **c** the difference between MOVE water tempera-ture and in situ observation by profiling float, **d** same as (**a**), except around 26–32°N, **e** same as (**b**), except around 26–32°N, and **f** same as (**c**), except around 26–32°N

(7052) is approximately 28.9 %. The number of records for TC deepening increases remarkably when MOVE-based TCHP exceeds 40 kJ cm^{-2}. The result supports the assumption that TCHP that exceeds the threshold plays an essential role in the increase in the occurrence of TC deepening.

3.3 Geographical factors

TCHP favorable for TC deepening is actually considered to vary depending on geographical factors such as latitude and longitude, as well as TC intensity and TC moving speed. This subsection addresses the relationship between MOVE-based TCHP before the passage of TCs and TC deepening for each geographical factor, TC intensity, and TC moving speed. The relationship was investigated for each domain every 5° in latitude from 5°N to 20°N and every 6° in latitude from 20°N to 32°N (Fig. 1). In addition, the relationship was investigated for each longitudinal domain; west of 120°E, east of 140°E and between 120°E and 140°E. West

of 120°E, a summer-monsoon circulation with a monsoon trough is dominant (Holland 1995) as atmospheric external forcing for TC deepening, whereas Pacific easterlies are predominant east of 140°E for tropical cyclogenesis (Ritchie and Holland 1999). The intermediate area (120–140°E) corresponds to a confluence region arising from a westerly jet with cross-equatorial flow, the Pacific easterly flow, an anticyclonic gyre to the northeast (Holland 1995; Ritchie and Holland 1999) and monsoon gyre (Lander 1994).

In this subsection, MOVE-based TCHP is briefly referred to as "TCHP". TCHP was categorized into the following six bins: 0–20, 20–40, 40–60, 60–80, 80–100, and above 100 kJ cm^{-2}. TC intensity was determined from the best-track central pressure and was categorized into the following six bins: below 920, 920–940, 940–960, 960–980, 980–1000, and above 1000 hPa. TC moving speed was calculated from the distance between the current and subsequent positions divided by 6 h. The TC moving speed was
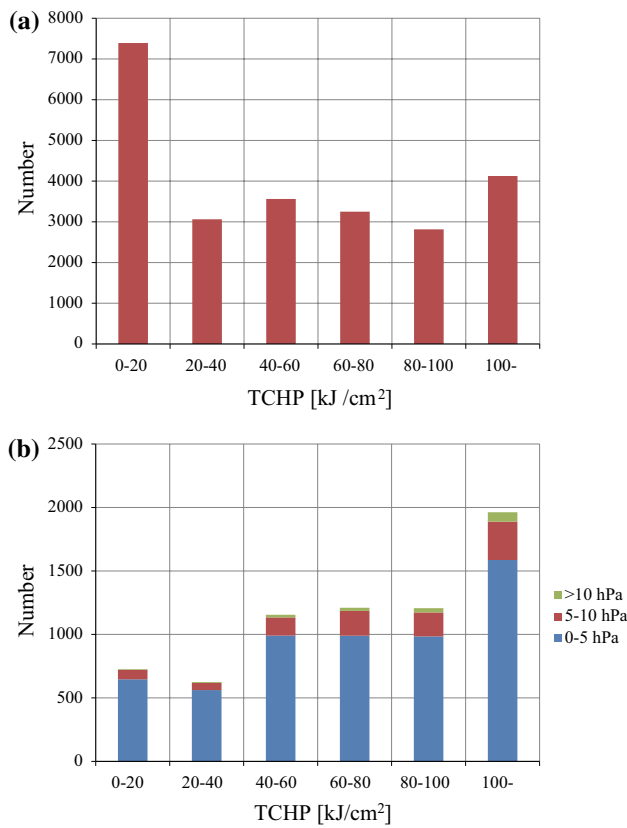
Fig. 6 **a** Histogram of the number of TCs for each TCHP bin every 20 kJ cm^{-2} using MOVE-based TCHP, **b** cumulative bar chart of the number of TCs, with deepening every 20 kJ cm^{-2} using MOVE-based TCHP

categorized into the following six bins: below 3, 3–5, 5–7, 7–9, 9–11, and above 11 m s^{-1}.

First, the ratio of the number of records for TC deepening to that of the total number of records is determined for each domain as the following reference ratio r_f (statistically corresponding to a population rate).

$$r_f = N_{\text{deepening}} / N_{\text{total}}, \tag{2}$$

where N_{total} is the total number of records and $N_{\text{deepening}}$ is the number of records for TC deepening. The reference ratio refers to the probability for the occurrence of TC deepening for each domain irrespective of TCHP values. Next, the ratios of the number of records for TC deepening ($N_{\text{d\_tchp}}$, $N_{\text{d\_cp}}$, $N_{\text{d\_spd}}$) to that of the total number of records ($N_{\text{t\_tchp}}$, $N_{\text{t\_cp}}$, $N_{\text{t\_spd}}$) are determined for each bin of TCHP (r_{tchp}), central pressure (r_{cp}) and moving speed (r_{spd}) as follows.

$$r_{\text{tchp}} = N_{\text{d\_tchp}} / N_{\text{t\_tchp}}, \tag{3}$$

$$r_{\text{cp}} = N_{\text{d\_cp}} / N_{\text{t\_cp}}, \tag{4}$$

$$r_{\text{spd}} = N_{\text{d\_spd}} / N_{\text{t\_spd}}. \tag{5}$$

Finally, the ratios of the number of records for TC deepening ($N_{\text{d\_cp\_tchp}}$, $N_{\text{d\_spd\_tchp}}$) to that of the total number of records ($N_{\text{t\_cp\_tchp}}$, $N_{\text{t\_spd\_tchp}}$) for each bin of central pressure ($r_{\text{cp\_tchp}}$) and moving speed ($r_{\text{spd\_tchp}}$) are determined for each TCHP bin.

$$r_{\text{cp\_tchp}} = N_{\text{d\_cp\_tchp}} / N_{\text{t\_cp\_tchp}}, \tag{6}$$

$$r_{\text{spd\_tchp}} = N_{\text{d\_spd\_tchp}} / N_{\text{t\_spd\_tchp}}. \tag{7}$$

Statistical significance is investigated for each ratio with reference to the reference ratio r_f based on the z-test. When the ratio for each TCHP bin exceeds the reference ratio at a significance level of 0.05, the TCHP value is regarded as a requisite condition for the increase in the occurrence of TC deepening. The minimum range of the TCHP value is regarded as the threshold of TCHP for the increase. The corresponding ratio r_{mintchp} is determined as follows.

$$r_{\text{mintchp}} = N_{\text{d\_mintchp}} / N_{\text{t\_mintchp}}, \tag{8}$$

where $N_{\text{t\_mintchp}}$ is the total number of records and $N_{\text{d\_mintchp}}$ is the number of records for TC deepening at the threshold of TCHP. It should be noted that a ratio with more than 20 TC deepening records (approximately two records per year) is used for examining statistical significance based on the z-test and determining the threshold.

Figure 7 shows bar charts indicating the ratio of TC deepening to the total number of TCs [i.e., the reference ratio r_f and the ratio for each TCHP threshold r_{mintchp} (Fig. 7a)], the ratio for each specified range of central pressure (r_{cp}) and the highest ratio (highest $r_{\text{cp\_tchp}}$) for each specified range of both central pressure and TCHP for each domain (Fig. 7b). It also shows bar charts indicating the ratio for each specified range of TC moving speed (r_{spd}) and the highest ratio (highest $r_{\text{spd\_tchp}}$) for each specified range of both TC moving speed and TCHP for each domain (Fig. 7c). The major characteristics are as follows: the reference ratio r_f is highest around 10–15°N and decreases north of 10°N as the latitude increases (Fig. 7a). This value is relatively high around 120–140°E.

Figure 7a indicates that TCs tend to intensify over relatively high-TCHP areas exceeding the threshold, except around 10–15°N. No threshold is statistically significant at the significance level of 0.05 around 10–15°N. The threshold is lowest (40–60 kJ cm^{-2}) around 5–10°N, west of 120°E and east of 140°E, whereas it is highest (80–100 kJ cm^{-2}) around 15–20°N. The threshold decreases as the latitude increases and the longitude decreases. The effect of TCHP exceeding the threshold on the increase in the occurrence of TC deepening is remarkable west of 120°E. The ratio of TC deepening increases significantly from r_f (0.22) to r_{mintchp} (0.38). Around 26–32°N, the threshold is 60–80 kJ cm^{-2}, which is higher than that around 5–10°N, west of 120°E and east of 140°E. However,

Fig. 7 Bar charts of **a** population rate (r_f) that best-track records indicate TC deepening among all TC records for each domain and ratio at the threshold of TCHP ($r_{mintchp}$) displayed on the *right side* of each *bar*; **b** a ratio at a certain central pressure (r_{cp}) and the highest ratio (highest r_{cp_tchp}) at a certain central pressure and that at a certain TCHP; and **c** a ratio at a certain moving speed (r_{spd}) and the highest ratio (highest r_{spd_tchp}) at a certain moving speed and that at a certain TCHP. The population rate (r_f) and the other ratios are significant at a significance level of 0.05 based on the z-test
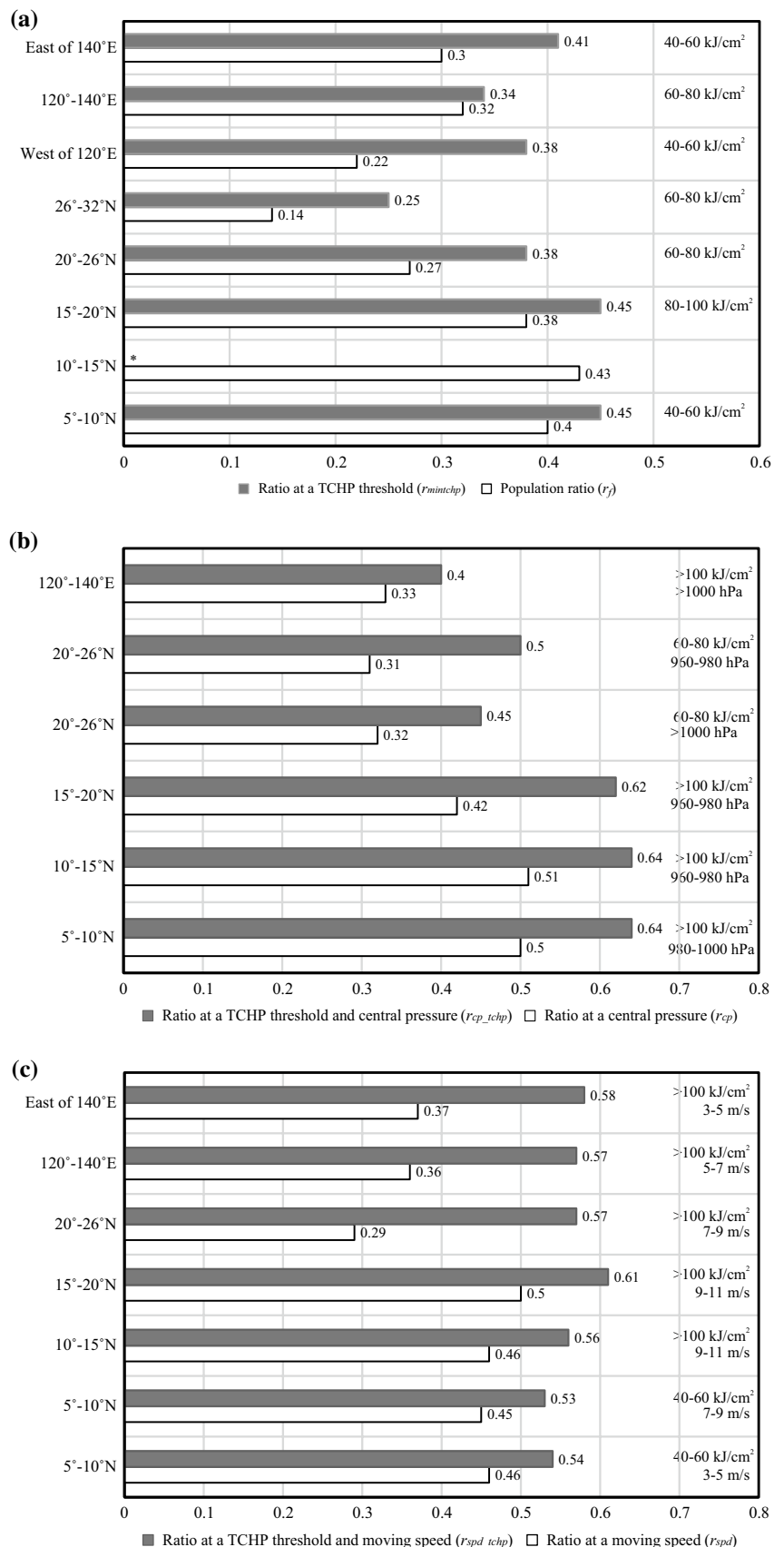
the ratio of TC deepening $r_{mintchp}$ is the lowest (0.25) of all domains. This means that only a quarter of all TCs intensify over the ocean, even if TCHP exceeds the threshold.

Figure 7b shows that TCs tend to intensify at a certain range of central pressure. The ratio of TC deepening increases over relatively high-TCHP areas at a significance level of 0.05. Around 5–20°N, TCs tend to intensify over relatively high-TCHP areas with values exceeding 100 kJ cm^{-2} when the central pressure favorable for the increase in the occurrence of TC deepening is relatively high (above 960 hPa; Fig. 7b). The ratio of TC deepening r_{cp_tchp} exceeds 0.6, which is approximately 0.1 higher than the ratio r_{cp} at the range of central pressure irrespective of TCHP. Around 120–140°E, the central pressure favorable for an increase in the occurrence of TC deepening exceeds 1000 hPa, indicating that relatively high TCHP helps storm cyclogenesis. Around 20–26°N, the value of TCHP (60–80 kJ cm^{-2}) is the same as the threshold value (Fig. 7a). In this domain, relatively weak TCs tend to intensify over TCHP areas with 60–80 kJ cm^{-2}.

Figure 7c shows that TCs tend to intensify in a certain range of moving speed. The ratio of TC deepening r_{spd_tchp} increases over relatively high TCHP areas at a significance level of 0.05. At around 5–10°N, the ratio of TC deepening r_{spd_tchp} for each moving speed shows two peaks: 40–60 kJ cm^{-2} with moving speeds of 3–5 and 7–9 m s^{-1}. The ratio increases by approximately 0.1 over the TCHP area with values of 40–60 kJ cm^{-2}. Around 10–26°N, around 120–140°E and east of 140°E, TCHP values exceeding 100 kJ cm^{-2} represent favorable conditions for the increase in the occurrence of TC deepening with relatively fast moving speeds (9–11 m s^{-1}) around 10–20°N and relatively slow moving speeds (3–5 m s^{-1}) east of 140°E. Therefore, TCHP values higher than the threshold are requisite conditions for the increase in the occurrence of TC deepening at a certain central pressure and moving speed. In addition, geographical factors should be considered in the use of the threshold of TCHP for TC intensity forecasts, because the ratio of TC deepening differs significantly among regions. Figure 7 also indicates that TC deepening is explained not only by TCHP alone, although relatively high values certainly contribute.

Lin et al. (2009b) reported that the slower (faster) the storm, the higher (lower) the TCHP value needs to be to realize the most intense TC. The present paper addresses the relationship between TC deepening defined by central pressure drops and MOVE-based TCHP before the passage of a TC. This study does not directly address the statistical relationships between the values of TC central pressure and TCHP/Z26.

It is well known that the ocean response to the most intense TC causes strong deepening of the mixed layer, resulting in TC-induced strong sea surface cooling when the pre-existing mixed layer is relatively shallow before the passage of the TC. Strong sea surface cooling leads to reduced sea-to-air turbulent heat fluxes, so that high TCHP and deep Z26 are needed as one of prerequisite conditions when the moving speed is relatively slow. It should be noted that this study does not take into consideration the effect of the ocean response to TCs and associated variation in TCHP values during the passage of TCs. Because the assimilation window of the MOVE system used in this study is 5 days, longer than the time scale of the ocean response to a TC, and the amplitude of the atmospheric wind stress is poor at producing a strong ocean response due to its relatively coarse horizontal resolution (0.5°), the ocean response could not be well analyzed in the present study. The development of an assimilation system will be expected in the future.

This discussion is not always valid when a relatively weak TC undergoes an early deepening around 10–20°N in the western Pacific where TCHP is climatologically high. Relatively fast moving speed can be favorable for producing an inflow layer and supergradient flow above the inflow layer (Smith et al. 2009), resulting in strong updrafts around the eyewall and convective bursts (Rogers et al. 2013) without decreasing the TCHP value. However, the ocean response to a TC plays a crucial role in changes in TCHP and TC intensity in the Subtropical Countercurrent region due to a large amount of sea surface cooling induced by TCs because of the relatively shallow mixed-layer depth. Around the region, warm ocean eddies essentially lead to a small amount of sea surface cooling, resulting in the increase in the occurrence of TC intensification.

3.4 TC intensification and maximum intensity around 5–10°N

Subsection 3.3 indicates that the geographical factor strongly affects the threshold of MOVE-based TCHP before the passage of TCs for the increase in the occurrence of TC deepening in the western North Pacific. In addition, this study finds for the first time that the region around 5–10°N is an exception: high MOVE-based TCHP does not contribute to the increase in the occurrence of TC deepening in all cases. Even though MOVE-based TCHP exceeds 100 kJ cm^{-2}, the ratio of the number of records for TC deepening to that of the total number of records is not statistically significant at a significance level of 0.05 when the central pressure is lower than 960 hPa, and the moving speed is lower than 3 m s^{-1} and higher than 9 m s^{-1} (not shown).

Figure 8 shows the seasonal variation in the number of occurrences of TC deepening for which central pressure drops are greater than 5 hPa. The number is notably highest in November, with relatively low TCHP and shallow
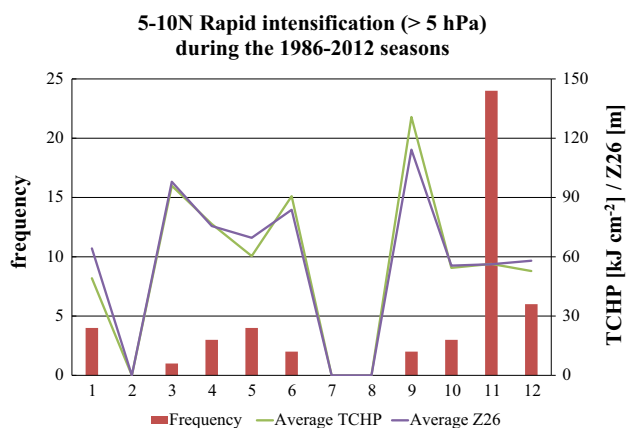
5-10N Rapid intensification (> 5 hPa) during the 1986-2012 seasons

Fig. 8 Seasonal variations in the frequency of rapid deepening for which the central pressure drop exceeded 5 hPa during the 1986–2012 years and in the monthly mean TCHP (kJ cm^{-2}) and Z26 (m)

Z26 calculated based on MOVE data, whereas there are no data in July and August. In this subsection, Typhoons Mike (1990) and Haiyan (2013) are exemplified to show the relation of TC deepening to moving speeds and TCHP around 5–10°N. It should be noted that TCHP and Z26 data below a TC are calculated based on the analysis day during the passage of the TC in this subsection.

Figure 9a displays the best tracks of Typhoons Mike and Haiyan. The tracks are quite similar to each other. However, the best-track central pressure, MOVE-based TCHP, and Z26 are quite different between Mike (Fig. 9b) and Haiyan (Fig. 9c). The average moving speed during the deepening of Mike from 6 to 10 November 1990 is approximately 5.2 m s^{-1}, whereas that of Haiyan from 4 to 6 November 2013 is approximately 8.4 m s^{-1}. During the deepening, the TCHP value is lower than 80 kJ cm^{-2} beneath Mike, whereas the TCHP value is higher than 120 kJ cm^{-2} below Haiyan. This indicates that Mike intensified over relatively low TCHP and slow movement around 5–10°N. The ratio of the number of records for TC deepening to that of the total number of records over the TCHP area with 60–80 kJ cm^{-2} is 0.45 with moving speeds of 5–7 m s^{-1}, while that exceeding 100 kJ cm^{-2} is 0.49 with moving speeds of 7–9 m s^{-1}. Both ratios are statistically significant at a significance level of 0.05. However, the duration of TC deepening exceeding 10 hPa for the nearest 6 hours clearly differed between Mike (18 h) and Haiyan (30 h) even though both TCs underwent rapid TC deepening in a similar way. The difference of duration did not affect the occurrence of TC intensification, but the maximum intensify of the two TCs.

Figure 10 shows the evolution of TCHP and Z26 derived from daily MOVE reanalysis data (Fig. 10a) and that of the difference between the 5-day TCHP and daily TCHP for Haiyan (Fig. 10b). The TCHP value is high during the

intensification, even though daily TCHP is used. The difference is relatively small and insignificant (lower than 10 kJ cm^{-2}) during the intensification phase of Haiyan, but becomes significantly large (higher than 25 kJ cm^{-2} at a statistical significance level of 0.1, based on the t test) during the mature phase at 1200 UTC on 8 November 2013, even though the average moving speed on 8 November is approximately 11.4 m s^{-1}, faster than the moving speed during the intensification. The error is approximately 10 kJ cm^{-2} between daily and 5-day TCHP products under the condition that Z26 is approximately 100 m, which corresponds to the change in water temperature of 0.2 °C above Z26. This is because Haiyan-induced sea surface cooling is relatively small due to the relatively fast moving speed of Haiyan.

The comparison between cases of Mike and Haiyan indicates that relatively high TCHP led to more rapid deepening exceeding 10 hPa for the nearest 6 hours during the intensification phase. In addition, relatively long duration resulted in an increased maximum intensity. The difference in best-track central pressures is greatest at the mature phase between Mike (915 hPa) and Haiyan (895 hPa). Here, the focus moves to the difference in the maximum intensity between Mike and Haiyan.

Previous studies indicate that it is not TCHP, but accumulated TCHP from the genesis of TCs to the attainment of maximum intensity that is highly correlated with TC maximum intensity (Wada and Usui 2007; Wada and Chan 2008; Wada 2009; Wada et al. 2012; Vissa et al. 2013). In addition, the temporal evolution of TC intensity is related to that of the horizontal specific humidity flux within the inner core of a TC in the lower troposphere, where inertial stability is relatively high (Wada et al. 2013). When the above-mentioned studies are taken into consideration, the accumulated TCHP, the duration over the positive TCHP region, is connected with the increase in horizontal specific humidity fluxes within the inner core of a TC in the lower troposphere through the excitation of mesovortices between the eye and the radius of maximum wind speed (Wada 2009). However, whether the difference in best-track central pressures between Mike (915 hPa) and Haiyan (895 hPa) can be explained only by the difference in the accumulated TCHP is beyond the scope of the present study.

Nevertheless, the difference in lower-tropospheric environments from 1990 to 2013 obtained from the JRA-55 data set will provide beneficial information for understanding the reason why the best-track central pressures differ between Mike and Haiyan. Figure 11 shows the time series of 13 monthly mean specific humidities and geopotential height at the 925 hPa level averaged over the area around 5–10°N and 125–150°E from 1985 to 2013. During this period, the mean specific humidity near the surface

Fig. 9 a Best tracks of
Typhoons Mike (1990)
(*squares*) and Haiyan (2013)
(*circles*) with central pres-
sures (*color shading*). **b** Time
series of central pressure (*right
vertical axis*), TCHP, and Z26
(*left vertical axis*) for Typhoon
Mike (1990). **c** Same as Fig. 9b,
except for Typhoon Haiyan
(2013)
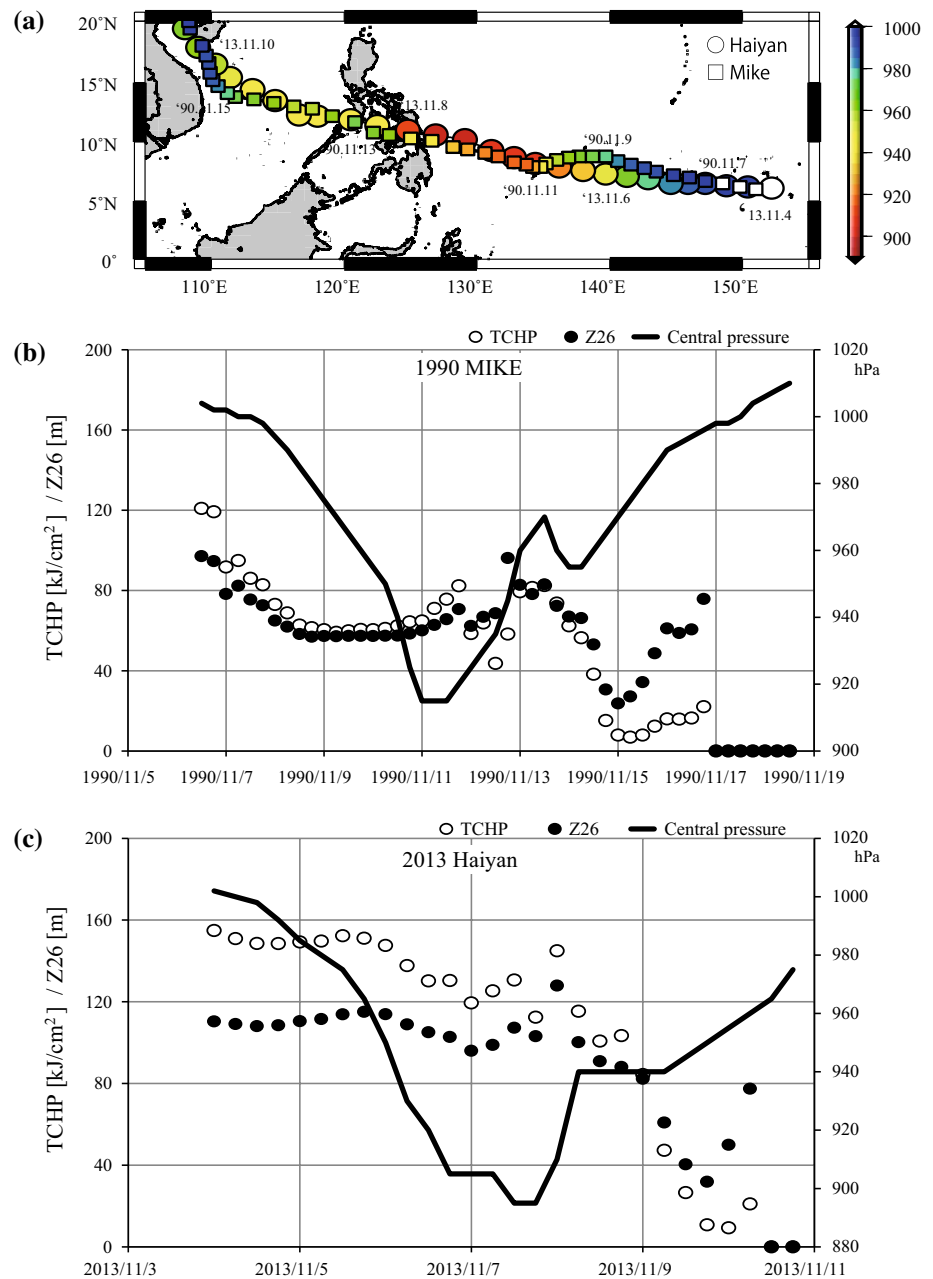
boundary layer significantly increased around the tracks
of Haiyan and Mike at a significant level of 0.01 based on
the *F*-test, whereas the mean geopotential height decreased
little. However, the process that connects the increase in
TCHP values with that in the specific humidity at 925 hPa
height has not yet been clarified. In any cases, atmospheric
environmental conditions, such as the moisture distribution
in the lower troposphere shown in Fig. 11, can be affected
by a change in the environmental TCHP distributions. The
effect of the environmental TCHP distribution on the physi-
cal processes of TC deepening through a change in atmos-
pheric environments, including the increase in specific

humidity in the lower troposphere, should be clarified in
the future.

4 Concluding remarks

To provide operational guidelines that include information
regarding the threshold of tropical cyclone heat potential
(TCHP) for improving tropical cyclone (TC) intensity fore-
casting in the western North Pacific, this study explored
the relationship between TCHP and TC deepening for TC
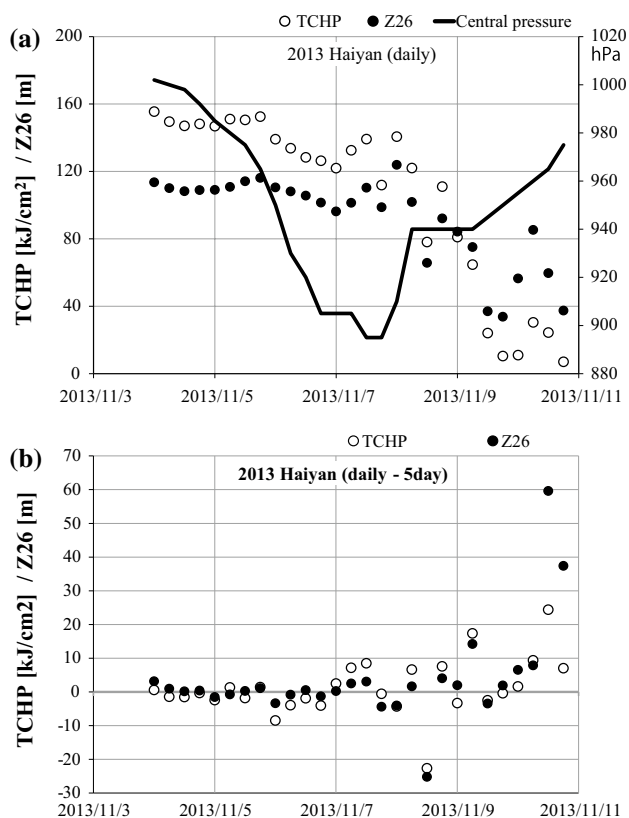moving speed, TC central pressure, and geographic factors

Fig. 10 a Same as Fig. 9c, except that the daily TCHP and Z26 are used. **b** The difference in TCHP (kJ cm^{-2}) and Z26 (m) values between the 5-day MOVE and daily MOVE
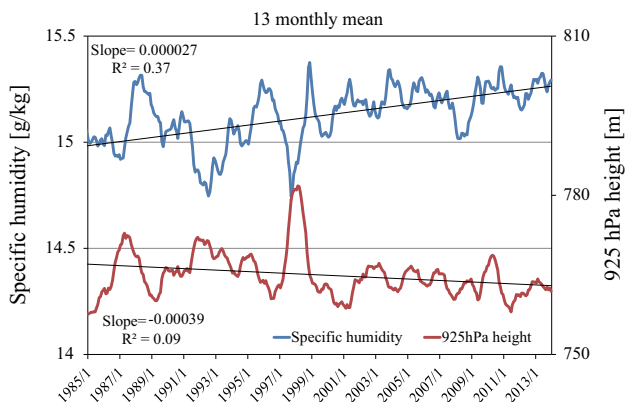

Fig. 11 Time series of the 13 monthly mean specific humidity and the geopotential height at the 925 hPa level averaged over the area around 5–10°N and 125–150°E from 1985 to 2013

such as longitude and latitude. TCHP is a measurable metric calculated by the summation of ocean heat content from the surface down to the depth of the 26 °C isotherm (Z26).

TCHP calculated by the North Pacific version of the Meteorological Research Institute multivariate ocean variational estimation (MOVE) system is verified using TCHP

based on in situ observations by profiling floats from 2002 to 2012. After 2008, MOVE-based TCHP becomes high compared to TCHP data before 2007 with reference to the TCHP value calculated from in situ observations. Around the seasonal thermocline, the positive bias of water temperature in the MOVE reanalysis has been remarkable since 2008, being responsible for the positive bias of MOVE-based TCHP. The lower the latitude is, the greater the impact of the difference in water temperature on the TCHP calculation.

After verification, the relationship between TCHP before the passage of a TC and TC deepening was investigated by using MOVE-based TCHP calculated based on 5-day mean ocean reanalysis data from 1985 to 2012. The ratio of the number of records with positive deviation $\Delta p_{6h} > 0$ hPa to the total number of records was 28.9 % during this period. This study examines the threshold of 5-day MOVE-based TCHP for the increase in the occurrence of TC deepening: TC deepening is defined by a positive deviation of the TC central pressure ($\Delta p_{6h} > 0$) for the nearest 6 hours at the corresponding TC record from that at the subsequent TC record. The reference ratio of the number of records for the occurrence of TC deepening to that of the total number of records irrespective of TCHP is determined at first. The reference ratio indicates the probability for the occurrence of TC deepening irrespective of TCHP. The ratio is calculated for each bin of central pressure, moving speed and the TCHP value. Statistical significance is examined for each ratio with reference to the reference ratio based on the z-test. When the ratio for each TCHP bin significantly exceeds the reference ratio, the TCHP value is regarded as a requisite condition for the increase in the occurrence of TC deepening. The minimum range of TCHP is regarded as the threshold of TCHP for the increase in this study.

The threshold is lowest (40–60 kJ cm^{-2}) around 5–10°N, west of 120°E, and east of 140°E, whereas it is highest (80–100 kJ cm^{-2}) around 15–20°N. The threshold decreases as the latitude increases and the longitude decreases. The effect of the threshold on the increase in the occurrence of TC deepening is remarkable west of 120°E: The ratio increases extremely from 0.22 to 0.38. Around 15–20°N, no threshold of TCHP is significant at a significance level of 0.05. The threshold is an index providing an essential condition for the increase in the occurrence of TC deepening: high TCHP value is requisite for the increase in the occurrence of TC intensification at a certain central pressure and moving speed. However, geographical factors should be considered to determine the threshold of TCHP in TC intensity forecasts.

Around 5–10°N, the ratio of the number of records for TC deepening to that of the total number of records is not significant at a significance level of 0.05 when the central pressure is lower than 960 hPa, the moving speed is

lower than 3 m s^{-1} and higher than 9 m s^{-1}, even though a MOVE-based TCHP exceeds 100 kJ cm^{-2}. This study addresses Typhoons Mike (1990) and Haiyan (2013) as case studies. Mike enables to intensify under a relatively low TCHP (<80 kJ cm^{-2}) and slow movement (nearly 5.2 m s^{-1}), although the maximum intensity was relatively weak compared with that of Haiyan under a relatively high TCHP (>120 kJ cm^{-2}) and fast movement (nearly 8.4 m s^{-1}). In fact, the duration of TC deepening exceeding 10 hPa for the nearest 6 hours for Mike (18 h) is shorter than that for Haiyan (30 h). TCHP derived from daily MOVE data was compared with 5-day MOVE-based TCHP. The results indicate that the difference between daily MOVE-based TCHP and 5-day MOVE-based TCHP, less than 10 kJ cm^{-2}, is not significant during the intensification phase, corresponding to the change in water temperatures approximately less than 0.2 °C above Z26. This is because Haiyan-induced sea surface cooling is relatively small due to the relatively fast moving speed of Haiyan.

When MOVE-based TCHP before the passage of a TC is used for monitoring TC deepening, not only the threshold for each latitudinal or longitudinal bin, but also that for each TC intensity or TC moving speed bin should be taken into consideration for monitoring TC intensity changes and TC intensity forecasts. It should be noted that the relationship between TCHP and TC maximum intensity is different from that between TCHP and TC deepening or TC intensification: The longer duration results in the greater amplitude of TC deepening due to an increase in accumulated TCHP, even if a TC begins to deepen even over the relatively low TCHP area.

References

Akima H (1970) A new method of interpolation and smooth curve fitting based on local procedures. J Assoc Comp Mach 17:589–602

Ali MM, Jagadeesh PSV, Jain S (2007) Effects of eddies on Bay of Bengal cyclone intensity. EOS Trans Am Geophys Union 88:93–99

Ali MM, Jagadeesh PSV, Lin I-I, Hsu JY (2012) A neural network approach to estimate tropical cyclone heat potential in the Indian Ocean. Geosci Remote Sens Lett IEEE 9(6):1114–1117

Ebita A, Kobayashi S, Ota Y, Moriya M, Kumabe R, Onogi K, Harada Y, Yasui S, Miyaoka K, Takahashi K, Kamahori H, Kobayashi C, Endo H, Soma M, Oikawa Y, Ishimizu T (2011) The Japanese 55-year Reanalysis "JRA-55": an interim report. SOLA 7:149–152

Gill AE (1982) Atmosphere–ocean dynamics, vol 30. Academic Press

Gjorgjievska S, Raymond DJ (2014) Interaction between dynamics and thermodynamics during tropical cyclogenesis. Atmos Chem Phys 14(6):3065–3082

Goni GJ, Trinanes JA (2003) Ocean thermal structure monitoring could aid in the intensity forecast of tropical cyclones. EOS Trans AGU 84(51):573–580

Goni G, Kamholz S, Garzoli S, Olson D (1996) Dynamics of the Brazil-Malvinas Confluence based on inverted echo sounders and altimetry. J Geophys Res Oceans 101(C7):16273–16289

Goni GJ, DeMaria M, Knaff J, Sampson C, Ginis I, Bringas F, Mavume A, Lauer C, Lin I-I, Ali MM, Sandery P, Ramos-Buarque S, Kang K, Mehra A, Chassignet E, Halliwell G (2009) Applications of satellite-derived ocean measurements to tropical cyclone intensity forecasting. Oceanography 22(3):176–183

Gray WM (1979) Hurricanes: Their formation, structure, and likely role in the tropical circulation. In: Shaw DB (ed) Meteorology over the tropical oceans. R Meteorol Soc, Bracknell, pp 155–218

Holland GJ (1995) Scale interaction in the western Pacific monsoon. Meteorol Atmos Phys 56:57–79

Ishikawa I, Tsujino H, Hirabara M, Nakano H, Yasuda T, Ishizaki H (2005) Meteorological Research Institute Community Ocean Model (MRI.COM) manual. Technical Reports of the Meteorological Research Institute 47, p 189 (in Japanese)

Knaff JA, DeMaria M, Sampson CR, Peak JE, Cummings J, Schubert WH (2013) Upper oceanic energy response to tropical cyclone passage. J Clim 26(8):2631–2650

Kumar B, Chakraborty A (2011) Movement of seasonal eddies and its relation with cyclonic heat potential and cyclogenesis points in the Bay of Bengal. Nat Hazards 59:1671–1689. doi:10.1007/s11069-011-9858-9

Lander MA (1994) Description of a monsoon gyre and its effects on the tropical cyclones in the western North Pacific during August 1991. Weather Forecast 9:640–654

Law K (2011) The impact of oceanic heat content on the rapid intensification of Atlantic hurricanes, recent hurricane research–climate, dynamics, and societal impacts, Lupo A (ed), ISBN: 978-953-307-238-8, InTech, doi:10.5772/13799

Leipper D, Volgenau D (1972) Upper ocean heat content of the Gulf of Mexico. J Phys Oceanogr 2:218–224

Lin I-I, Wu C-C, Emanuel KA, Lee I-H, Wu C-R, Pan I-F (2005) The interaction of supertyphoon Maemi (2003) with a warm ocean eddy. Mon Weather Rev 133:2635–2649. doi:10.1175/MWR3005.1

Lin I-I, Chen CH, Pun I-F, Liu WT, Wu C-C (2009a) Warm ocean anomaly, air sea fluxes, and the rapid intensification of tropical cyclone Nargis (2008). Geophys Res Lett 36(3):L03817. doi:10.1029/2008GL035815

Lin I-I, Pun I-F, Wu C-C (2009b) Upper ocean thermal structure and the western North Pacific category-5 typhoons. Part II: dependence on translation speed. Mon Weather Rev 137:3744–3757

Mainelli M, DeMaria M, Shay LK, Goni G (2008) Application of oceanic heat content estimation to operational forecasting of recent Atlantic category 5 hurricanes. Weather Forecast 23:3–16. doi:10.1175/2007WAF2006111.1

Malan N, Reason CJC, Loveday BR (2013) Variability in tropical cyclone heat potential over the Southwest Indian Ocean. J Geophys Res Oceans 118(12):6734–6746. doi:10.1002/2013JC008958

Pun IF, Lin II, Wu CR, Ko DS, Liu WT (2007) Validation and application of altimetry-derived upper ocean thermal structure in the western North Pacific Ocean for typhoon intensity forecast. IEEE Trans Geosci Remote Sens 45:1616–1630

Pun IF, Lin I-I, Lo MH (2013) Recent increase in high tropical cyclone heat potential area in the Western North Pacific Ocean. Geophys Res Lett 40(17):4680–4684

Pun IF, Lin I-I, Ko DS (2014) New generation of satellite-derived ocean thermal structure for the Western North Pacific typhoon intensity forecasting. Prog Oceanogr 121:109–124

Ritchie EA, Holland GJ (1999) Large-scale patterns associated with tropical cyclogenesis in the western Pacific. Mon Weather Rev 127:2027–2043

Rogers R, Reasor P, Lorsolo S (2013) Airborne Doppler observations of the inner-core structural differences between intensifying and steady-state tropical cyclones. Mon Weather Rev 141:2970–2991

Shay LK (2010) Air-sea interactions in tropical cyclones. In: Chan JCL, Kepert JD (eds) Global perspective on tropical cyclones from science to mitigation. World Scientific, Singapore, pp 93–132

Shay LK, Brewster JK (2010) Oceanic heat content variability in the eastern Pacific Ocean for hurricane intensity forecasting. Mon Weather Rev 138(6):2110–2131. doi:10.1175/2010MWR3189.1

Shay LK, Goni GJ, Black PG (2000) Effects of a warm oceanic feature on hurricane Opal. Mon Weather Rev 128:1366–1383

Smith RK, Montgomery MT, Van Sang N (2009) Tropical cyclone spin-up revisited. Q J R Meteorol Soc 135:1321–1335

Typhoon Hai-Tang in 2005. Adv Meteorol 2010:756071. doi:10.1155/2010/756071

UNESCO (1981) Tenth report of the joint panel on oceanographic tables and standards. UNESCO Technical Papers in Marine Sci. 36. UNESCO, Paris

Usui N, Ishizaki S, Fujii Y, Tsujino H, Yasuda T, Kamachi M (2006) Meteorological Research Institute multivariate ocean variational estimation (MOVE) system: some early results. J Adv Space Res 37:806–822. doi:10.1016/j.asr.2005.09.022

Vissa NK, Satyanarayana ANV, Kumar BP (2013) Intensity of tropical cyclones during pre-and post-monsoon seasons in relation to accumulated tropical cyclone heat potential over Bay of Bengal. Nat Hazards 68(2):351–371. doi:10.1007/s11069-013-0625-y

Wada A (2009) Idealized numerical experiments associated with the intensity and rapid intensification of stationary tropical-cyclone-like vortex and its relation to initial sea-surface temperature and vortex-induced sea-surface cooling. J Geophys Res 114:D18111. doi:10.1029/2009JD011993

Wada A, Chan JCL (2008) Relationship between typhoon activity and upper ocean heat content. Geophys Res Lett 35:L17603. doi:10.1029/2008GL035129

Wada A, Usui N (2007) Importance of tropical cyclone heat potential for tropical cyclone intensity and intensification in the Western North Pacific. J Oceanogr 63:427–447

Wada A, Usui N (2010) Impacts of oceanic preexisting conditions on predictions of

Wada A, Usui N, Sato K (2012) Relationship of maximum tropical cyclone intensity to sea surface temperature and tropical cyclone heat potential in the North Pacific Ocean. J Geophys Res 117:D11118. doi:10.1029/2012JD017583

Wada A, Usui N, Kunii M (2013) Interactions between Typhoon Choi-wan (2009) and the Kuroshio Extension System. Adv Meteorol 2013:859810. doi:10.1155/2013/859810

Wang Y, Wu C-C (2004) Current understanding of tropical cyclone structure and intensity changes-a review. Meteorol Atmos Phys 87:257–278

Wang B, Zhou X (2008) Climate variation and prediction of rapid intensification in tropical cyclones in the western North Pacific. Meteorol Atmos Phys 99:1–16. doi:10.1007/s00703-006-0238-z